



# The Zero Bias Schottky Diode Detector at Temperature Extremes – Problems and Solutions

## Application Note 1090

### Abstract

The zero bias Schottky diode detector is ideal for RF/ID tag applications where it can be used to fabricate a receiver which consumes no primary power. However, its performance is heavily dependent upon its saturation current, which is a strong function of temperature. At both low and high temperature extremes, this dependence can lead to degradation in performance. The behavior of zero bias Schottky diodes is analyzed, experimental data is given, and a solution to the loss of performance at cold temperatures is presented.

### Introduction

The zero bias Schottky diode detector [1], [2] is widely used in RF/ID and other applications where no primary (DC) power is available in the standby or “listen” mode. When combined with a simple antenna to form a receiver, it lacks the sensitivity of the superheterodyne receiver, but offers the advantages of very low cost and zero power consumption. The single diode detector is shown in Figure 1.

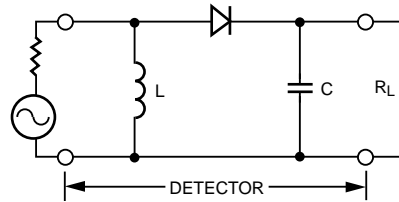


Figure 1. Diode Detector

$R_L$  is the video load resistance.  $L$ , the shunt inductance, provides a current return path for the diode, and is chosen to be large (compared to the diode's impedance) at the input or RF frequency.  $C$ , the bypass capacitance, is chosen to be sufficiently large that its capacitive reactance is small compared to the diode's impedance but small enough to avoid having its reactance load the video circuit [3].

Such detector circuits display a characteristic transfer curve of output voltage vs. input power as shown in Figure 2.

$P_{in}$  is the RF input power applied to the detector circuit and  $V_o$  is the output voltage appearing across  $R_L$ . As can be seen from Figure 2, the transfer curve follows a square law (output voltage proportional to the square of input voltage) at low levels of input

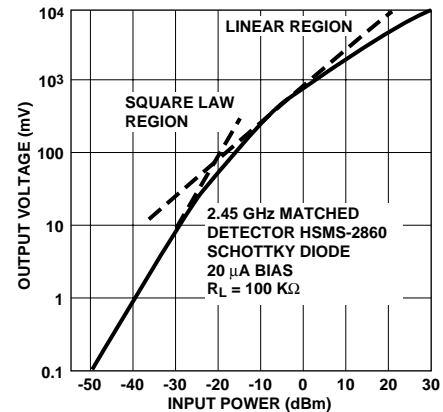


Figure 2. Detector Transfer Curve

power and displays quasi-linear behavior (output voltage proportional to input voltage) at higher levels.

A key performance criterion for a diode detector is the slope of the transfer curve,  $\gamma$ , generally expressed in mV/ $\mu$ W. One can plot  $\gamma$  vs.  $P_{in}$  as shown in Figure 3.

Such a plot is a more sensitive indicator of detector performance than the transfer plot of Figure 2. Note that  $\gamma$  is a function of externally applied bias (among other parameters) in conventional (DC biased) detectors. It can be noted from Figure 3 that external bias can be adjusted to trade sensitiv-

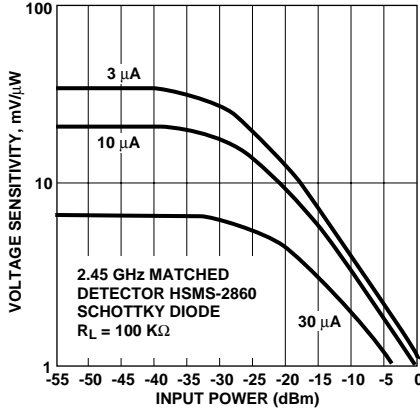


Figure 3.  $\gamma$  vs. Input Power

ity for a wider dynamic range of square law response.

A Schottky diode can be represented by the linear equivalent circuit shown in Figure 4.

$L_p$  is package parasitic inductance.  $C_p$  is package parasitic capacitance.  $R_s$  is the diode's parasitic series resistance.  $C_j$  is junction parasitic capacitance and  $R_j$  is the diode's junction resistance.

Figures 1 and 4 can be combined to create both an RF and video equivalent circuit of the Schottky diode detector. The RF equivalent circuit is given in Figure 5.

Note that this equivalent circuit does not include the RF impedance matching network which is normally found between the diode and the 50  $\Omega$  source.

Figure 6 shows the video equivalent circuit for the diode detector, where  $C_T$  is the sum of bypass capacitance and input capacitance of the video circuit.

$L_p$ ,  $C_p$ , and  $R_L$  are constants.  $R_s$  has some small variation with temperature, but that variation is

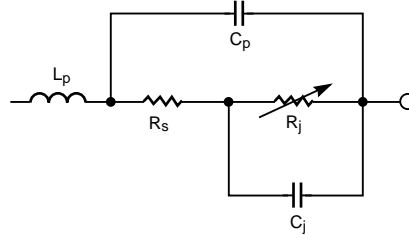


Figure 4. Diode Equivalent Circuit

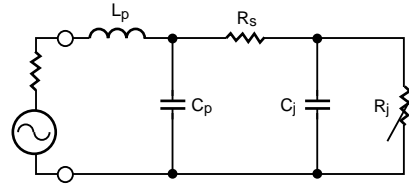


Figure 5. RF Equivalent Circuit of a Detector

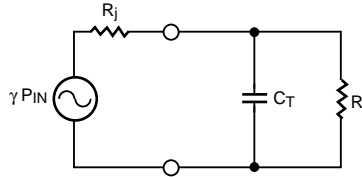


Figure 6. Video Equivalent Circuit of a Detector

not a significant parameter in this analysis.  $C_j$  is a function of both temperature and DC bias, but this analysis concerns itself with the zero bias detector and the variation with temperature is not significant.  $R_j$  is a key element in both equivalent circuits — its behavior clearly will affect the performance of the detector circuit.

While many commercial applications cover a narrower temperature range, the analysis which follows will include the 140° from -55° to +85°C.

### Junction Resistance

Three different currents affect the junction resistance of a Schottky diode. The first is the diode's own saturation current,  $I_s$ . The second is externally applied bias current,

$I_o$ . The third is  $I_c = V_o/R_L$ , the circulating current produced by rectification in the diode. In the small signal region of interest in this discussion, where  $I_c < I_s$ , the equation for junction resistance is:

$$R_j = \frac{n k T}{q (I_s + I_o)} \quad (1)$$

where  $n$  is the diode ideality factor (emission coefficient),  $k$  is Boltzmann's constant ( $1.38062 \times 10^{-23}$  Joules/°K),  $q$  is the electronic charge ( $1.60219 \times 10^{-19}$  Coulomb), and  $T$  is temperature in degrees Kelvin.

The equation for saturation current is given by:

$$I_s = I_{s0} \left( \frac{T}{T_0} \right)^{\frac{2}{n}} e^{-\frac{q\psi}{k} \left( \frac{1}{T} - \frac{1}{T_0} \right)} \quad (2)$$

where  $T_0$  is 273°K (room temperature),  $I_{s0}$  is saturation current measured at room temperature and  $\psi$  is the metal-semiconductor Schottky barrier height (energy gap).

Combining these two equations produces a relation for  $R_j$  as a function of temperature.

For a high performance zero bias Schottky detector, such as the Agilent Technologies HSMS-2850,  $I_{s0} = 3 \mu A$ ,  $n = 1.2$  and  $\psi = 0.35$  eV. Using these values in (1) and (2) results in the computed junction resistance shown in Figure 7.

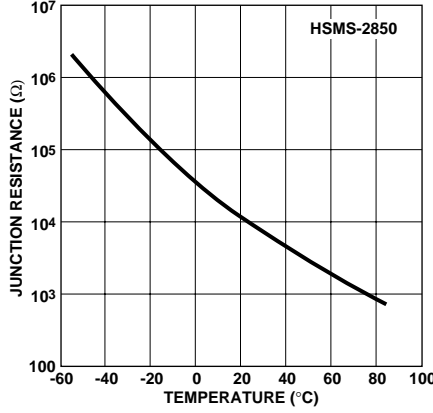


**Figure 7.  $R_j$  vs. Temperature for the HSMS-2850**

As can be seen from this figure,  $R_j$  varies by three and a half decades over the 140°C temperature range.

This variation in  $R_j$  will affect two performance parameters of vital interest to the detector circuit designer.

## Performance Over Temperature

### Schottky Diode

The two performance parameters of interest to the circuit designer are the video bandwidth and voltage sensitivity of the detector. The analysis of video bandwidth as a function of temperature is straightforward [3] and will be shown first.

The video equivalent circuit shown in Figure 6 has a low pass filter response, with a 3 dB cutoff frequency defined by

$$f_c = \frac{1}{2 \pi C_T R_T} \quad (3)$$

where

$$R_T = \frac{R_j R_L}{R_j + R_L} \quad (4)$$

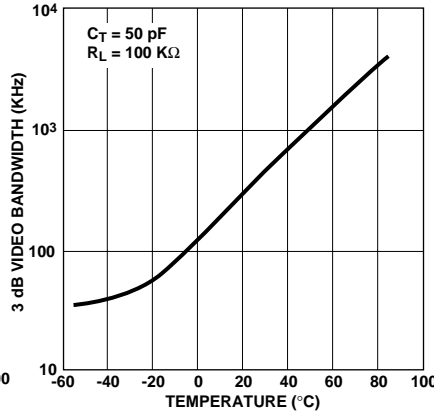


**Figure 8.  $f_c$  vs. Temperature for the HSMS-2850**

Using the variation in  $R_j$  given in Figure 7, the variation in video bandwidth can be computed. Typical values of  $R_L = 100 \text{ K}\Omega$  and  $C_T = 50 \text{ pF}$  were used to compute the curve of cutoff frequency vs. temperature shown in Figure 8.

As can be seen from this plot, video bandwidth can shrink to a value as low as 30 KHz at -55°C. Many RF/ID systems [4] use data rates which are higher than 30 KHz. Of course, a reduction in  $C_T$  will improve bandwidth, but there are practical limits to how low total capacitance can be made. Similarly, a reduction in  $R_L$  will increase video bandwidth, but at the expense of voltage sensitivity, according to the following relationship.

$$\gamma = \gamma_{oc} \frac{R_L}{R_L + R_j} \quad (5)$$

where  $\gamma$  is the detector's voltage sensitivity for  $R_L = \text{infinity}$ .

The analysis of voltage sensitivity as a function of temperature for a Schottky diode detector is complex. Harrison and Le Polozec [5] have provided an exact analysis for zero frequency, as shown in Equation 6 below.

In Equation 6,  $I_o$  is the zero-order modified Bessel function of the first kind,  $P_{inc}$  is the incident RF power,  $R_g$  is the generator or source resistance,  $\Lambda = q/kT$ . This equation can be solved for  $P_{inc}$  as a function of  $V_o$  using Mathcad(1) and the work-sheet shown in [6].

An examination of Equation (6) will reveal that only  $\Lambda$  and  $I_s$  are functions of temperature, aside from the small variation of  $R_s$  mentioned earlier. This equation can be applied to a zero bias Schottky diode, such as the HSMS-2850, terminating a 50  $\Omega$  source as shown in Figure 1. Curves of voltage sensitivity vs. input power and temperature can then be calculated as shown in Figure 9.

Due to the choice of the optimum value for  $I_{so}$  [2], the diode shows reasonable sensitivity at 25°C (despite the lack of an RF impedance matching network) and good square law response

(1) Product of MathSoft, Inc., 201 Broadway, Cambridge, Massachusetts

$$I_o \left( \frac{\Lambda}{n} \sqrt{8 R_g P_{inc}} \right) = \left( 1 + \frac{I_o}{I_s} + \frac{V_o}{R_L I_s} \right) \left[ \left( 1 + \frac{R_g + R_s}{R_L} \right) \frac{\Lambda}{n} V_o + \frac{\Lambda}{n} R_s I_o \right] \quad (6)$$

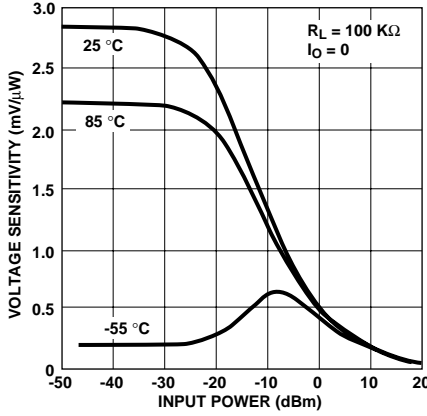


Figure 9.  $\gamma$  vs.  $P_{in}$  and Temperature for the HSMS-2850 at zero frequency

(flat  $\gamma$ ) almost to -30 dBm. At 85°C,  $I_s$  has increased beyond the optimum, and sensitivity suffers slightly. However, behavior at -55°C does not follow traditional models; sensitivity peaks at -8 dBm, and drops off to less than half the peak value at small signal levels where detectors are most often used. This anomalous effect is the consequence of the very low value of  $I_s$  at -55°C.

While a powerful and convenient tool, Equation (6) neglects the effects of diode junction capacitance, package parasitics and RF input matching network, all of which are part of practical diode detectors.

#### Detector Diode and Circuit

In [1], several detector designs with RF impedance matching networks are presented, along with test data obtained at 25°C. The 2.45 GHz single-diode detector designed around the 25°C characteristics of the HSMS-2850 device was chosen for further analysis and test over temperature.

An analysis tool [7] was created to add the effects of frequency and reactive circuit elements to Equation (6). This tool was applied to

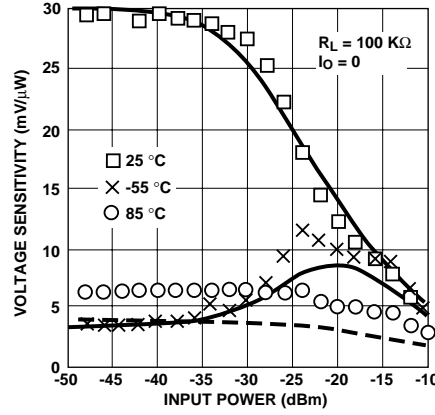


Figure 10.  $\gamma$  vs.  $P_{in}$ , 2.45 GHz Detector

the 2.45 GHz detector and the resulting data were compared to performance measured on a prototype circuit. Calculated and measured data are shown in Figure 10.

In this figure, the top curve is the calculated sensitivity at 25°C, which is compared to the measured data (indicated by boxes). The middle curve and "X" marks compare calculated and measured at -55°C. The bottom curve and circles compare calculated and measured at 85°C. Note that in this case, where a RF input impedance transformer has been placed between source and diode, voltage sensitivity is ten times greater at 25°C. However, sensitivity drops rapidly at 85°C, compared to the unmatched case shown in Figure 9. Agreement between calculated and measured is good except for the data at 85°C. As in the zero frequency case shown in Figure 9, performance at -55° is anomalous, except that the effect of the RF input matching network was to shift the peak value of  $\gamma$  from -8 dBm down to -22 dBm.

A more common diode detector measurement is output voltage vs.

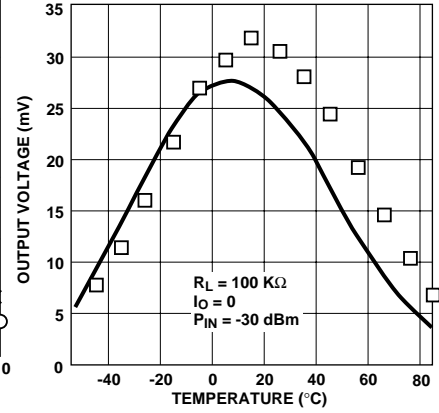


Figure 11. Output Voltage vs. Temperature, 2.45 GHz Detector

temperature at some fixed value of input power. Such data were obtained for the experimental circuit with  $P_{in} = -30$  dBm, and are compared to a calculated curve in Figure 11.

As was the case in Figure 10, agreement between predicted performance and experimental data is good except at higher temperatures.

An examination of (2) and (6) will show that variation in  $I_s$  with temperature is larger and more significant than the variation in  $\Lambda$ . Not only does the temperature sensitivity of  $I_s$  directly affect  $\gamma$  as given in (6), but it results in wide swings in  $R_j$ , as was seen in Figure 7. This, in turn, can change the input impedance match and result in substantial impedance mismatch losses at temperature extremes. Calculated input match for the 2.45 GHz detector under discussion is given in Figure 12. Circles on the Smith Chart are impedances given at 10° increments.

The design of the input impedance matching transformer was done at 25°C. From this figure, it can be seen that the input match is fairly good until temperature exceeds

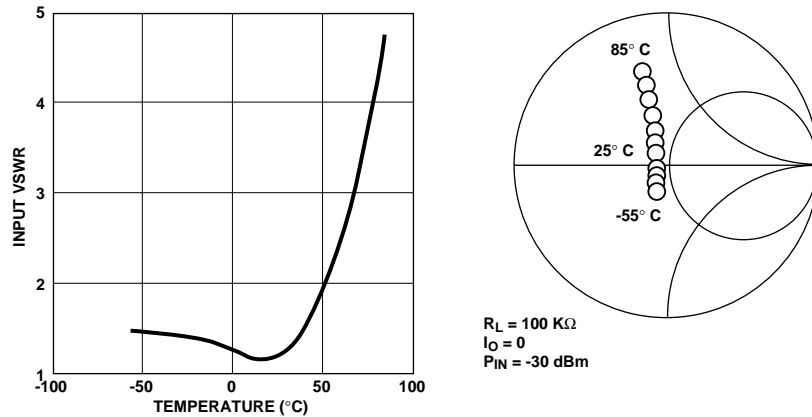


Figure 12. Calculated  $Z_{in}$  vs. Temperature, 2.45 GHz Detector

50°, after which it degrades quickly. Severe mismatch losses at the input to the detector are the result, lowering the power delivered to the diode's junction.

Because the impedance at high temperatures swings out from the origin of the Smith Chart so rapidly, a small error in modeling the impedance matching network can lead to errors in the prediction of high temperature sensitivity. This accounts for the difference between measured and predicted in Figure 11. However, a sensitivity analysis of the matching network is beyond the scope of this paper.

It can be seen that loss of video bandwidth and voltage sensitivity at cold temperatures is due to very low values of saturation current, leading to a drop in performance as predicted by (3) and (6). At high temperatures, RF impedance mismatch losses at the input to the detector lead to loss of sensitivity. These two different problems suggest two different solutions.

## Compensation Methods

### Low temperature compensation:

Conventional DC biased detectors generally operate from a continuous current of 10 to 30  $\mu\text{A}$ , and offer greater temperature stability than the zero bias Schottky detector. However, these are devices with saturation currents in the nanoamp range. Nevertheless, the use of supplemental DC bias current suggests itself as a solution to poor video bandwidth and low sensitivity at low temperatures.

The 2.45 GHz detector described in Figures 10, 11 and 12 was tested with small amounts of supplemental DC bias, as shown in Figure 13.

It can be seen that less than 1  $\mu\text{A}$  of current can compensate for loss of sensitivity at cold temperatures. An examination of Figure 13 suggests that 0.5  $\mu\text{A}$  of supplemental bias current would produce a flat output voltage from  $-55^\circ$  to  $15^\circ\text{C}$ .

At temperatures above  $20^\circ\text{C}$ , these small amounts of external bias current have virtually no effect on output voltage.

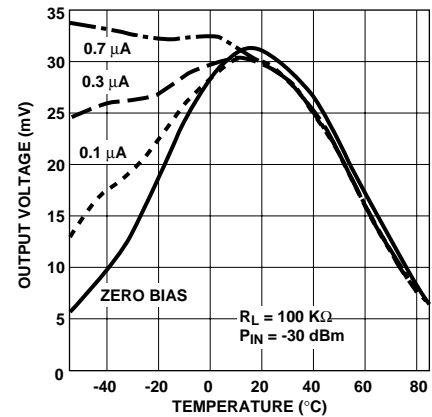


Figure 13. Measured  $V_O$  vs. Temperature, 2.45 GHz Detector

An analysis was performed of the small signal transfer curve of this detector at  $-55^\circ\text{C}$  as a function of external DC bias, as shown in Figure 14.

It can be seen that a supplemental DC bias of 0.5  $\mu\text{A}$  dramatically brings up the voltage sensitivity in the small signal region, nearly eliminating the anomalous behavior observed at zero bias.

In addition, this small DC bias prevents junction resistance from exceeding 43  $\text{K}\Omega$  at temperatures below  $-20^\circ\text{C}$ , raising the 3 dB video bandwidth below this temperature to a minimum of 100 KHz (refer to Figure 8).

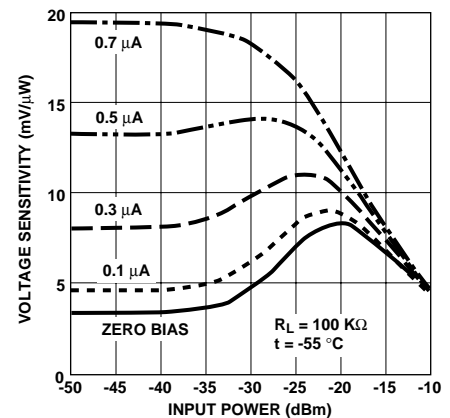


Figure 14. Calculated Transfer curve, 2.45 GHz Detector

### High Temperature Compensation

As was seen in Figure 12 and from comparing Figures 9 and 10, RF impedance mismatch is the major cause for poor voltage sensitivity at 85°C.

To compensate for poor sensitivity at 85°C, the input matching network for the 2.45 GHz detector under discussion was redesigned. Calculated input parameters for this high temperature detector are shown in Figure 15.

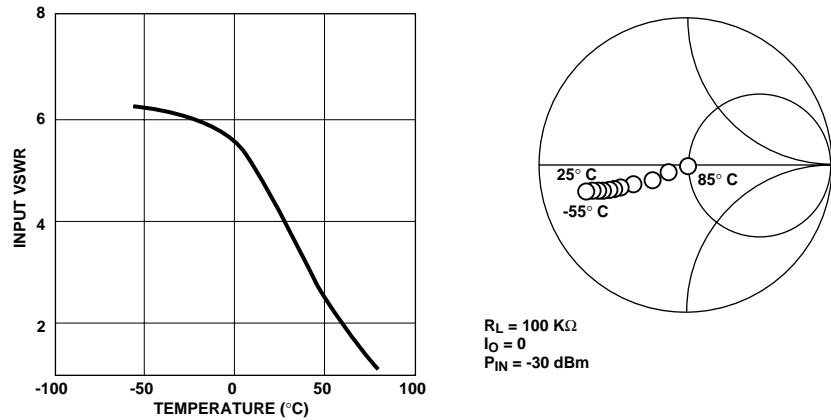


Figure 15. Calculated  $Z_{in}$  vs. Temperature, redesigned 2.45 GHz detector

In this case, care was taken to provide a perfect match at 85°C, allowing the match at other temperatures to degrade. This approach contrasts sharply to the impedance behavior given in Figure 12. Output voltage vs. temperature was then calculated for this new design, as shown in Figure 16.

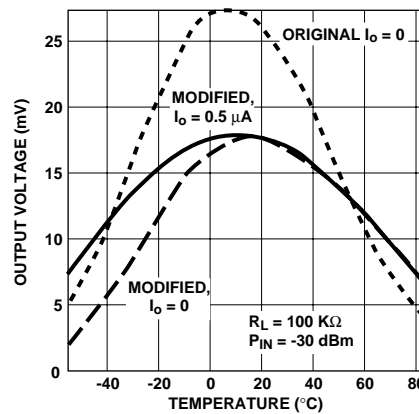


Figure 16. Output Voltage vs. Temperature, redesigned 2.45 GHz detector

Three plots are given in this figure. The first (dotted line) is the output voltage at zero bias for the original design (a copy of the data from Figure 11). The second (dashed line) is the zero bias output voltage for the redesigned matching network described in Figure 15. The third (solid line) is that same matching network, but with 0.5  $\mu\text{A}$  of supplemental bias added. It can be seen from comparing the dashed and dotted plots that changing the RF impedance transformer raised the output voltage at 85°C and reduced it at temperatures under 55°C. The tradeoff for this temperature compensation is lower output voltage at room temperature.

The addition of 0.5  $\mu\text{A}$  of supplemental bias had no practical effect on output voltage for temperatures over 20°C, but brought

it up at -55°C. Because the RF impedance mismatch is so poor at -55°C in this revised design, additional supplemental bias would be required to completely compensate output voltage at cold temperatures.

The ratio of output voltage at 25°C to that at 85°C went from 6.9 (dotted line, Figure 16) to 2.7 (solid line) because of the design change. That ratio can be further reduced, but at the expense of sensitivity at room temperature. Referring to Figure 15, this can be done by moving the impedance match at 85°C to the left along the

real axis (towards the zero resistance point).

This approach to the temperature compensation of the Schottky diode detector works as well at any other RF frequency. The remaining discussion will focus on methods of controlling or limiting the supplemental bias current.

## Bias Control

A simple way to obtain a supplemental bias current is with a DC voltage source and a resistor. This is similar to conventional DC biased detector diodes except with a lower bias current level, as shown in Figure 17.

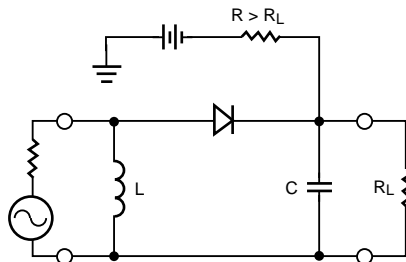


Figure 17. DC Biased Detector

If a 5 V battery is used in series with a 10 M $\Omega$  resistor, a bias current of 0.5  $\mu$ A will be supplied, increasing the output voltage at low temperatures as shown in Figure 16. In many tag designs with READ/WRITE capability, a 5 volt power source is readily available. The 10 M $\Omega$  resistor value does not load down the video circuit whose load resistor  $R_L$  is typically 1 K $\Omega$  - 100 K $\Omega$ . However, this current flow will be continuous and would shorten the battery (and tag) life. In addition, bias current has no practical effect at temperatures greater than 20°C. Thus, bias control that is temperature dependent is needed.

## Thermistor with Positive Temperature Coefficient

By replacing the 10 M $\Omega$  resistor in Figure 17 with a thermistor that has a positive temperature coefficient (PTC), the supplemental bias current would decrease at higher temperatures where it is not needed (to save battery life) and increase at lower temperatures to improve performance.

The AIRPAX Series 5024 Thermistors have a PTC characteristic as depicted in Figure 18.

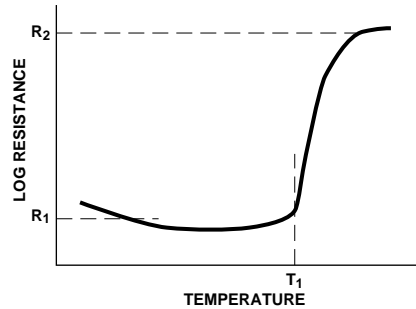


Figure 18. Typical PTC Thermistor

By specifying that  $R_1 = 10$  M $\Omega$ ,  $R_2 = 100$  M $\Omega$ , and  $T_1 = 10^\circ\text{C}$ , the 0.5  $\mu$ A of bias current would flow when  $T < 10^\circ\text{C}$ , and only 50 nA would flow when  $T > 10^\circ\text{C}$ . Other values of  $R_1$ ,  $R_2$ , and  $T_1$  can be selected to achieve optimum tag performance at specific temperature ranges.

## Power Supply with Thermostat

Using a thermistor, some current still flows even though it is not needed. Replacing the thermistor with a thermostat whose ON/OFF state is dependent on temperature, the bias current can be completely shut off so that no primary power is consumed at the higher temperatures (Figure 19). Note that the use of a low resistance thermostat requires the use of the 10 M $\Omega$  resistor seen in Figure 17.

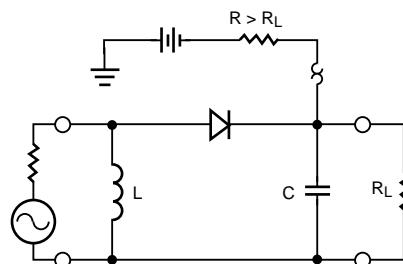


Figure 19. Detector with Thermostat

A snap action, bimetal disc switch such as the AIRPAX Series 5003 Thermostat can be used to turn the bias current on or off at different temperature set points. These switches are very reliable whose contact operation can be designed to close (open) when the temperature is decreasing (increasing) through a specified setpoint. This supplies the bias current only when needed so that no current is flowing at higher temperatures. Although these thermostats add cost to the circuit, the user may find that the performance and maintenance benefits outweigh these costs.

IC switches are also available that are temperature dependent. However, most require a supply voltage to operate and may have significant current levels even in the OFF position.

## Conclusion

The effects of temperature upon the performance of the zero bias Schottky diode detector have been analyzed and compared to experimental data. Two methods of compensation, for low and high temperature extremes, have been described.



## References

- [1] Raymond W. Waugh, "Designing Detectors for RF/ID Tags," *Proceedings of RF Expo West*, 1995, pp 212 - 223.
- [2] Rolando R. Buted, "Zero Bias Detector Diodes for the RF/ID Market," *H.P. Journal*, December 1995, pp 94 - 98.
- [3] Agilent Technologies Application Note 923, *Schottky Barrier Diode Video Detectors*.
- [4] Lawrence Livermore Labs, *An Automatic Vehicle ID System for Toll Collecting*, Lawrence Livermore National Laboratory LLNL Transportation Program, L-644
- [5] Robert G. Harrison and Xavier Le Polozec, "Nonsquarelaw Behavior of Diode Detectors Analyzed by the Ritz-Galérkin Method," *IEEE Transactions on Microwave Theory and Techniques*, Vol. 42, No. 5, May 1994, pp. 840 - 845.
- [6] Raymond W. Waugh, "Designing the Virtual Battery," *Proceedings of the WIRELESS Symposium*, 1995, pp 160 - 168.
- [7] Raymond W. Waugh, "A Model of the Schottky Diode Detector," to be published at a future date.